Original Article

JCBFM

Journal of Cerebral Blood Flow & Metabolism
0(0) 1–12

DOI: 10.1177/0271678X251326871
journals.sagepub.com/home/jcbfm
Sage

Therapeutic mitochondria treatment amplifies macrophage-mediated phagocytosis and recycling exocytosis

Masayoshi Tanaka[1], Shin Ishikane[1,2], Dong Bin Back[1], Ester Licastro[1,3], Fang Zhang[1], Ji Hyun Park[1], Elga Esposito[1], Giuseppe Pignataro[3], Takafumi Nakano[1,4], Yoshihiko Nakamura[1,5] and Kazuhide Hayakawa[1]

Abstract

Therapeutic administration of mitochondria has been increasingly explored. However, how these administered mitochondria impact immune response remains to be fully addressed. In this proof-of-concept study, we show that extracellularly added mitochondria to cultured peritoneal macrophages increase phagocytosis and recycling exocytosis that amplifies neuroplasticity mediated by recycled mitochondria transfer. Macrophage activation markers such as *Nos2*, *Arg1*, and *Cd163* were unchanged at 3 h post-treatment with mitochondria, but whole mitochondria or delivery of mRNAs extracted from whole mitochondria appeared to increase SQSTM1 protein and activate Nrf2-mediated phagocytosis in macrophages, whereas mitochondria treatment did not change the ability of phagocytosis in cultured microglia or astrocytes. Notably, the once engulfed mitochondria in macrophages appear to be released via Rab27a-mediated recycling pathway that were favorably incorporated in mechanically damaged neurons compared with healthy neurons, resulting in accelerating neurite extension in damaged neurons in a direct co-culture model. Altogether, these findings uncover unappreciated mechanisms that mitochondria-treated macrophages upregulate phagocytosis and recycling exocytosis, implicating that engineering mitochondria delivery to macrophages is a new therapeutic intervention to promote neurorecovery in CNS disorders.

Keywords

Therapeutic mitochondria, macrophages, SQSTM1/p62, Rab27a, neurons

Received 9 November 2024; Revised 17 February 2025; Accepted 24 February 2025

Introduction

For the vast majority of eukaryote cells, mitochondria are essential for maintaining metabolic homeostasis and regulating intracellular mechanisms that modulate viability, immune cell activation, and mitophagy.[1,2] Additionally, it has been recognized that mitochondria may play an important role in controlling gene expression profile and inducing signaling pathways by releasing more signal components into the cytoplasm or utilizing mitochondrial outer membrane as a translational platform.[3]

In the past decades, emerging evidence implicates that mitochondria are surprisingly transferred or exchanged between cells. The intercellular cell-to-cell signaling pathway was initially discovered in an in

[1]Neuroprotection Research Laboratories, Departments of Radiology and Neurology, Massachusetts General Hospital and Harvard Medical School, Charlestown, MA, USA
[2]Department of Pharmacology, School of Medicine, University of Occupational and Environmental Health, Fukuoka, Japan
[3]Division of Pharmacology, Department of Neuroscience, Reproductive and Dentistry Sciences, School of Medicine, University of Naples Federico II, Naples, Italy
[4]Department of Physiology and Pharmacology, Faculty of Pharmaceutical Sciences, Fukuoka University, Fukuoka, Japan
[5]Department of Emergency and Critical Care Medicine, Fukuoka University Hospital, Fukuoka, Japan

Corresponding author:
Kazuhide Hayakawa, Neuroprotection Research Laboratories, MGH East 149-2401, Charlestown, MA 02129, USA.
Email: khayakawa1@mgh.harvard.edu

vitro cell culture system wherein mtDNA from human mesenchymal progenitor cells (hMSCs) was delivered to A549 cells.[4] Since then, horizontal mitochondria transfer through various intercellular connections has been discovered in diverse physiological and pathological conditions in mammals.[5–7] Surprisingly, extracellular intact and functional mitochondria are present in healthy rodent and human,[8,9] implicating that mitochondria are now considered to play a role in both intracellular and extracellular homeostasis. However, what remains missing is how administered mitochondria influence macrophage-mediated innate immune response.

In this proof-of-concept study, we demonstrated that extracellularly added mitochondria were engulfed by macrophages without inductions of macrophage activation markers but increased SQSTM1 protein, Nrf2-mediated phagocytosis and Rab27a-mediated recycling exocytosis for extending neurites in vitro. Our study uncovered a new mechanism of macrophage response to extracellular mitochondria that can be the potential target to accelerate macrophage-mediated neurorecovery via peripheral administration of therapeutic mitochondria in CNS injury or disease.

Material and methods

Primary cultures

Primary neuron cultures were prepared from cerebral cortices of E18-day-old Sprague-Dawley rat embryos. Briefly, cortices were dissected and dissociated using papain dissociation system (Worthington Biochemical Corporation, LK003150). Cells were spread on plates coated with poly-D-lysine (Sigma, P7886) and cultured in Dulbecco's modified Eagle medium (NBM, Life Technology, 11965-084) containing 25 mM glucose, 4 mM glutamine, 1 mM sodium pyruvate, and 5% fetal bovine serum at a density of 2×10^5 cells/mL (1 mL for 12 well format, 0.5 mL for 24 well format). At 24 hrs after seeding, the medium was changed to Neurobasal medium (Invitrogen, 21103-049) supplemented with B-27 (Invitrogen, 17504044) and 0.5 mM glutamine. Cells were cultured at 37°C in a humidified chamber of 95% air and 5% CO_2. Over 95% of purity of neuron cultures was determined by MAP2 staining in our previous study. Macrophages were isolated from rat peritoneal cavity. After collecting cells from the cavity, cells were seeded on non-coated 6-well or 96-well plates and grown in RPMI medium 1640 containing 10% FBS, 1% penicillin/streptomycin. Five days later, attached cells were used for further experiment. For astrocyte and microglia isolation, cerebral cortices from 1–2 day old Sprague-Dawley rats were dissected, minced, and digested. Dissociated cells were plated in poly-D-lysine-coated 75-cm^2 flasks, and maintained in Dulbecco's Modified Eagle's medium containing 20% heat-inactivated fetal bovine serum (FBS) and 1% penicillin/streptomycin. After the cells were confluent (~10 days), the flasks were shaken for 1 hour on an orbital shaker (220 rpm) at 37°C to remove microglia. Non-adherent cells were collected as microglia following shaking the flasks and cultured in DMEM/F12 containing 10% FBS. Twenty-four hours later, microglia culture was used for further stimulation or experiment. After shaking the flasks for 1 hour, the medium was changed with a new medium and shaken overnight (~20 hrs). The cells were then collected and plated for culturing astrocytes.

Experiments were approved by the Mass General Brigham Institutional Animal Care and Use Committee (IACUC) and were performed under institutionally approved protocol in accordance with the National Institute of Health's Guide for the Care and Use of Laboratory Animals. All experiments were performed following an institutionally approved protocol in accordance with National Institutes of Health guidelines and with the United States Public Health Service's Policy on Human Care and Use of Laboratory Animals and following Animals in Research: Reporting In vivo Experiments (ARRIVE) guidelines.

Mitochondrial isolation

Mitochondria-enriched fractions were isolated from cryopreserved placenta, liver, spleen, heart, lung, kidney, brain, and skeletal muscle of Sprague-Dawley rats using a stepwise centrifugation method, ensuring that all procedures were conducted at 4°C to maintain mitochondrial integrity. First, the mitochondrial isolation buffer was prepared, consisting of 10 mM HEPES (pH 7.5), 25 mM sucrose, 1 mM ATP, 0.1 mM ADP, 5 mM sodium succinate, and 2 mM K_2HPO_4. Next, tissue samples were thawed on ice and rinsed with ice-cold mitochondrial isolation buffer to remove blood and contaminants. Then, the tissue was transferred to a pre-chilled glass-glass tissue grinder containing 1 mL of mitochondrial isolation buffer. Afterward, homogenization was performed using 20–30 strokes of a tight-fitting glass rod to ensure thorough mechanical disruption while minimizing mitochondrial damage. The homogenate was subsequently subjected to a series of centrifugation steps. Initially, centrifugation at 1,000 g for 5 minutes at 4°C was performed to remove cellular debris and nuclei. The supernatant was then centrifuged at 4,000 g for 5 minutes at 4°C to remove some larger organelles, such as fragments of the Golgi apparatus and partially sedimented lysosomes. The resulting supernatant was then centrifuged at 8,000 g for 10 minutes at 4°C, yielding a mitochondrial-enriched pellet. The final pellet was

resuspended in PBS to achieve a protein concentration of 1 μg/μL, as determined by bradford protein assay, using gentle pipetting to ensure uniform suspension, and stored on ice for immediate use.

mRNA isolation

Total RNA, including mitochondrial mRNA, was extracted from mitochondria-enriched fractions using the RNeasy Micro Kit (QIAGEN) according to the manufacturer's protocol. After mitochondrial isolation, the mitochondrial pellet was resuspended in 350 μL of RLT buffer, supplied with the kit, and supplemented with 1% β-mercaptoethanol to ensure complete lysis of mitochondria and inactivation of RNases. The sample was then homogenized by pipetting up and down 10 times, followed by vortexing for 30 seconds to enhance mitochondrial membrane disruption. To facilitate RNA binding to the silica membrane in the RNeasy spin column, the lysate was mixed with an equal volume of 70% ethanol (350 μL). The mixture was then transferred to the spin column and centrifuged at 8,000 g for 15 seconds at room temperature, allowing the RNA to bind efficiently to the membrane. To remove contaminants such as proteins and residual DNA, the column was first washed with 500 μL of RW1 buffer. Subsequently, on-column DNase I treatment was performed by adding 80 μL of DNase incubation buffer, followed by incubation at room temperature for 15 minutes to eliminate genomic DNA contamination. The column was then washed twice with 500 μL of RPE buffer to further improve RNA purity. The purified RNA was eluted using 14 μL of RNase-free water and immediately stored at −80°C for further analysis.

Mitochondria membrane potential measurement

To monitor mitochondrial health, Tetramethylrhodamine (TMRM) (invitrogen, T-668) was used to assess mitochondrial membrane potential. Macrophages were incubated with TMRM (100 nM) for 30 min at 37°C. Mitochondria membrane potential was determined by microplate reader with the absorbance peak at 548 nm and emission peak at 574 nm.

Oxygen consumption analysis

Real time basal oxygen consumption rate in isolated mitochondria were measured by Oxygen Consumption Rate Assay kit (Cayman Chemicals, 600800) according to the instruction provided by Cayman Chemicals. Briefly, macrophages or the conditioned media were prepared in clear bottom black 96 well plates, and oxygen sensor probe (10 μL) was added into each well. After covering with 100 μL of Oil, the plate were read with filter combination of 340 nm for excitation and 642 nm of emission at 30°C in a kinetic program.

E. coli phagocytosis assay

Rat peritoneal macrophages, rat primary microglia or rat primary astrocytes were treated with placental mitochondria (20 μg) for 24 hours prior to phagocytosis assay. The heat-inactivated green fluorescent-labeled E.coli (Abcam, ab235900) was added to cells for 3 hours then cells were washed twice with PBS to remove free floating E.coli. Phagocytosis ability was analyzed by the plate reader at Ex/Em at 490/520 nm.

mRNA encapsulation with DOTAP/DOPE

To encapsulate mRNAs extracted from isolated placental mitochondria, the inverted emulsion method was used. mRNA suspensions containing 1% polyvinyl alcohol was mixed with 100 μL of mineral oil containing 1 mM DOTAP/DOPE (1:1), followed by generating water/oil (W/O) emulsion by gently pipetting 10 times. The W/O emulsion was transferred onto 150 μL of mineral oil containing 1 mM DOTAP/DOPE (1:1) on 500 μL of PBS prepared in 1.5 mL tube at least 30 minutes before adding W/O emulsion. Five minutes after slowly adding W/O emulsion, the test tubes were spinned by the centrifugation at 12,000 g for 10 minutes at 4°C. Supernatant was discarded and the pellet was carefully resuspended in mitochondria buffer and washed one time with a centrifugation at 12,000 g for 10 minutes at 4°C.

Western blot analysis

Each sample was loaded onto 4–20% Tris-glycine gels. After electrophoresis and transferring to nitrocellulose membranes, the membranes were blocked in Tris-buffered saline containing 0.1% Tween 20 and 0.2% I-block (Tropix, T2015) for 90 min at room temperature. Membranes were then incubated overnight at 4°C with following primary antibodies, anti-β-actin (1:1,000, Sigma-aldrich A5441), anti-SQSTM1 (1:500, Thermo Fisher Scientific, PA5-20839), total OXPHOS rodent WB antibody cocktail (1:200, Abcam, ab110413). After incubation with peroxidase-conjugated secondary antibodies, visualization was enhanced by chemiluminescence (GE Healthcare, NA931- anti-mouse, or NA934- anti-rabbit, or NA935- anti-rat). Optical density was assessed using the NIH Image analysis software.

FACS analysis

Standard FACS analysis was performed by BD Fortessa 20. Macrophage-conditioned media were collected from rat peritoneal macrophages followed by filtrating

through a 1.2-μm syringe filter, WFACS analysis were performed using a variety of controls including unstained samples, isotype antibodies and single stained samples for determining appropriate gates, voltages, and compensations required in multivariate flow cytometry.

Statistical analysis

Results were expressed as mean ± SD. In vitro experiments were performed in duplicate or triplicate or sample-combined depending on the assay sensitivity, repeated at least 3 times independently. Sample size was predetermined using the software available online: https://www.danielsoper.com/statcalc/calculator.aspx?id=47. The calculation was based on Cohen's d value where SD and average were estimated from our historical and preliminary data. When only two groups were compared, Student's t-test was used. Multiple comparisons were evaluated by Tukey's test after one-way or two-way ANOVA. $p < 0.05$ was considered to be statistically significant. All experiments and analyses were conducted in a randomized and blinded manner in accordance with NIH guidelines on rigor and reproducibility.

Results

Mitochondria isolation from cryopreserved placenta and titration of the treatment

Mitochondria were isolated from rat placenta at the stage of embryonic E17 and evaluated total OXPHOS protein expressions. Consistent with our prior experiments,[10] isolated mitochondria highly expressed prototypical mitochondrial OXPHOS proteins including NDUFB8 (complex I), SDHB (complex II), UQCRC2 (complex III), MTCO1 (complex IV), and ATP5A (complex V) (Figure 1(a)). At 3 h after the treatment, we confirmed that fluorescent-labeled mitochondria were incorporated into most macrophages when the protein amount of mitochondrial fraction was 20 μg (Figure 1(b) and (c)) and we decided to use 20 μg protein of isolated mitochondria fraction for further experiments. Other parameters such as cell morphology (Figure 1(d)), viability (Figure 1(e) and (f)), mitochondrial membrane potential (Figure 1(g)), and basal oxygen consumption (Figure 1(h)) were not altered by the uptake of extracellular mitochondria in macrophages.

Mitochondria-driven SQSTM1 upregulation in peritoneal macrophages

Next, we further evaluated gene expressions related to macrophage phenotype (Figure 2(a)). At 3 hours post-mitochondria treatment, there were no significant changes in genes regulating macrophage activation (*Nos2*, *Arg1, Cd163*), lysosome-associated membrane proteins (*Lamp1, Lamp2*) and lysosomal function regulators (*Atg5, Ptpn2*) (Figure 2(b)), whereas *Sqstm1* known as an autophagy-related gene were significantly increased in macrophages (Figure 2(b)). Consistently, Western blot confirmed that SQSTM1 protein level was upregulated by the treatment with mitochondria at 24 hours (Figure 2(c)) and this may be partly induced by direct mRNA transfer because placental mitochondria carried *Sqstm1* mRNA (Figure 2(d)). To address it, we encapsulated mRNAs extracted from isolated placental mitochondria in engineered DOTAP/DOPE liposomes[11] (Figure 2(e)). Our engineered liposomes were efficiently incorporated into macrophages, delivered mRNA, and induced EGFP expression (Figure 2(f)). Notably, mitochondria-carrying mRNA delivery into macrophages increased SQSTM1 protein at 24 hours post-treatment (Figure 2 (g)). Besides placental mitochondria, *Sqstm1* mRNA was detected in various tissue-derived mitochondria fractions (Figure 2(h)), implicating that mitochondria-carrying mRNAs may have a potential to regulate cellular function and be engineered for the delivery into cells.

Treatment with mitochondria increases Nrf2-mediated phagocytosis in macrophages

SQSTM1 or p62 or sequestome 1 is evolutionally conserved and affects longevity and health. It is known that the KIR domain of SQSTM1 directly binds to Keap1 which releases and activates Nrf2 which is a prototypical phagocytosis regulator in macrophages (Figure 3(a)).[12,13] Notably, mitochondria treatment clearly increased Nrf2 fluorescent intensity in macrophages at 24 hours post-treatment (Figure 3(b) and (c)). To assess functional relevance of the increase of Nrf2 in macrophages, we next evaluated phagocytosis of fluorescent-labeled E.Coli particles. We initially confirmed the ability to incorporate E.Coli particles in rat peritoneal macrophages, rat primary microglia, and rat primary astrocytes (Figure 3(d)). Then, placental mitochondria were added onto rat peritoneal macrophages for 24 hours and the ability of incorporating *E.Coli* particles was evaluated at 3 hours after the exposure (Figure 3(e)). Interestingly, mitochondria-treated macrophages increased phagocytosis, whereas Nrf2 inhibition by co-treatment with ML385 diminished the effect (Figure 3(f)). Moreover, mitochondrial mRNA-loaded particles consistently amplified Nrf2-dependent phagocytosis ((Figure 3(g) and (h)). However, mitochondria treatment did not increase Nrf2-dependent phagocytosis in our routinely cultured brain microglia (Figure 3(i) and (j)) or astrocytes

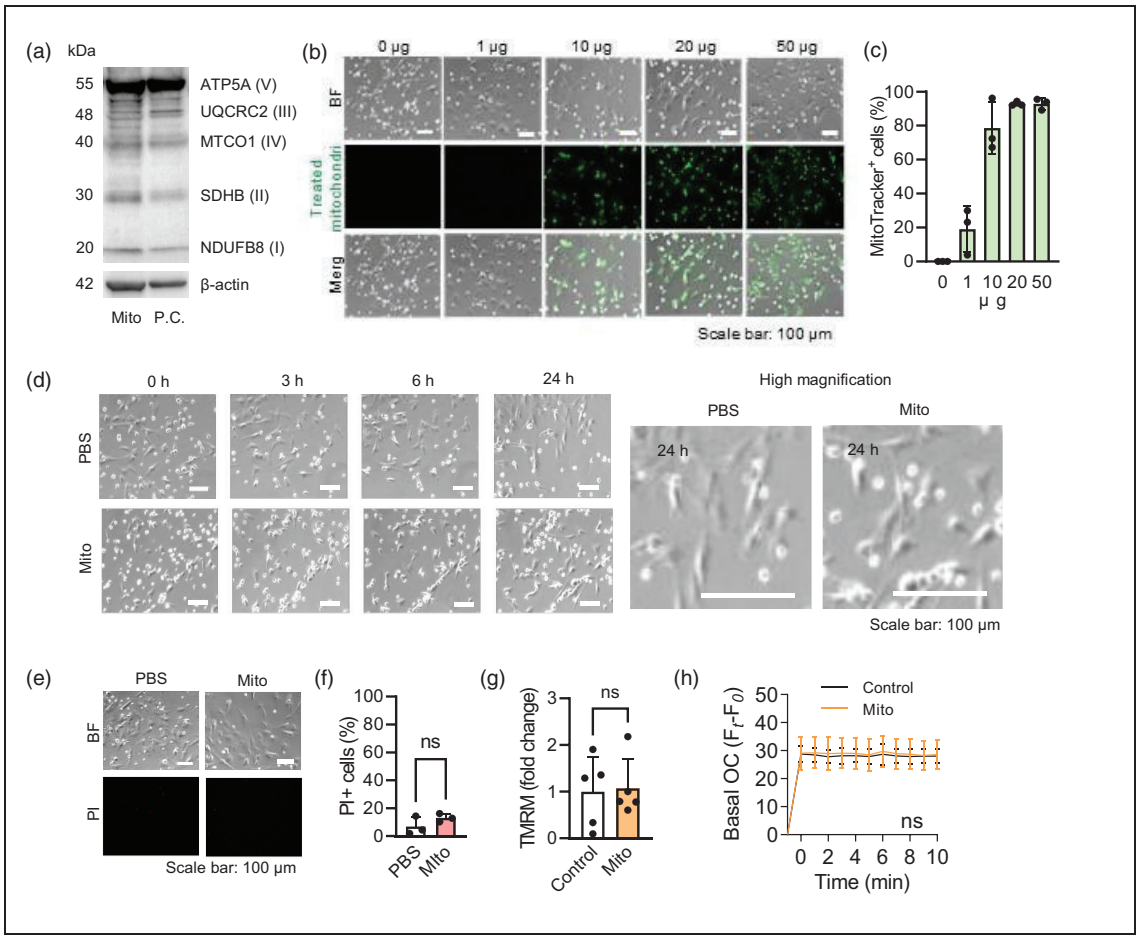

Figure 1. Mitochondria isolation and titration of the treatment. (a) Mitochondria were isolated from rat placenta and Western blot confirmed the successful isolation. P.C. positive control: rat heart mitochondria control: ab110413, Abcam. (b–c) Fluorescent signals at 3 h after MitoTracker Deep Red-labeled mitochondria treatment in rat peritoneal macrophages. Quantification showed that mitochondrial protein 20 μg were incorporated in over 90% of cultured macrophages (n = 3). (d) Treatment with mitochondria (20 μg) did not change macrophage shapes compared with untreated macrophages. (e–f) Treatment with mitochondria (20 μg) did not increase propidium iodide (PI) positive cells. Quantification of PI positive cells showed no difference between untreated control and mitochondria treatment (n = 3). (g) Mitochondrial membrane potential measured by TMRM showed no difference between untreated control and mitochondria treatment (n = 5) and (h) mitochondrial oxygen consumption showed no difference between untreated control and mitochondria treatment (n = 3). All data are shown as mean ± SD. ns, no significance.

(Figure 3(k) and (l)). Collectively, mitochondria-treated macrophages boosted the phagocytosis ability in a Nrf2-dependent manner.

Rab27a regulates recycling exocytosis in mitochondria-treated macrophages

So far, our data demonstrated that mitochondria-treated macrophages upregulated SQSTM1 and their phagocytosis activity. Traditionally, phagocytosis leads to a major reorganization of the plasma membrane and expanding the cell surface area accompanied by the exocytosis of intracellular compartments.[14] Additionally, it has been implicated that cargo receptor such as SQSTM1 can be associated with Rab27a which is functionally required for cargo receptor secretion upon lysosome inhibition.[15] Therefore, we first assessed the localization of engulfed mitochondria in the context of Rab27a-mediated exocytosis. Intriguingly, immunocytochemistry revealed that engulfed mitochondria appeared to be packed in vacuole-like vesicles which expressed SQSTM1 and Rab27a in macrophages (Figure 4(a)). If Rab27a mediates exocytosis, are engulfed mitochondria released from macrophages? To address this question, we analyzed extracellular mitochondria in culture media under Rab27a inhibition with nexinhib 20 and defined the composition of macrophage-originated mitochondria, fused mitochondria, and engulfed mitochondria by flow cytometry (Figure 4(b)). Extracellular particles less than 1 μm

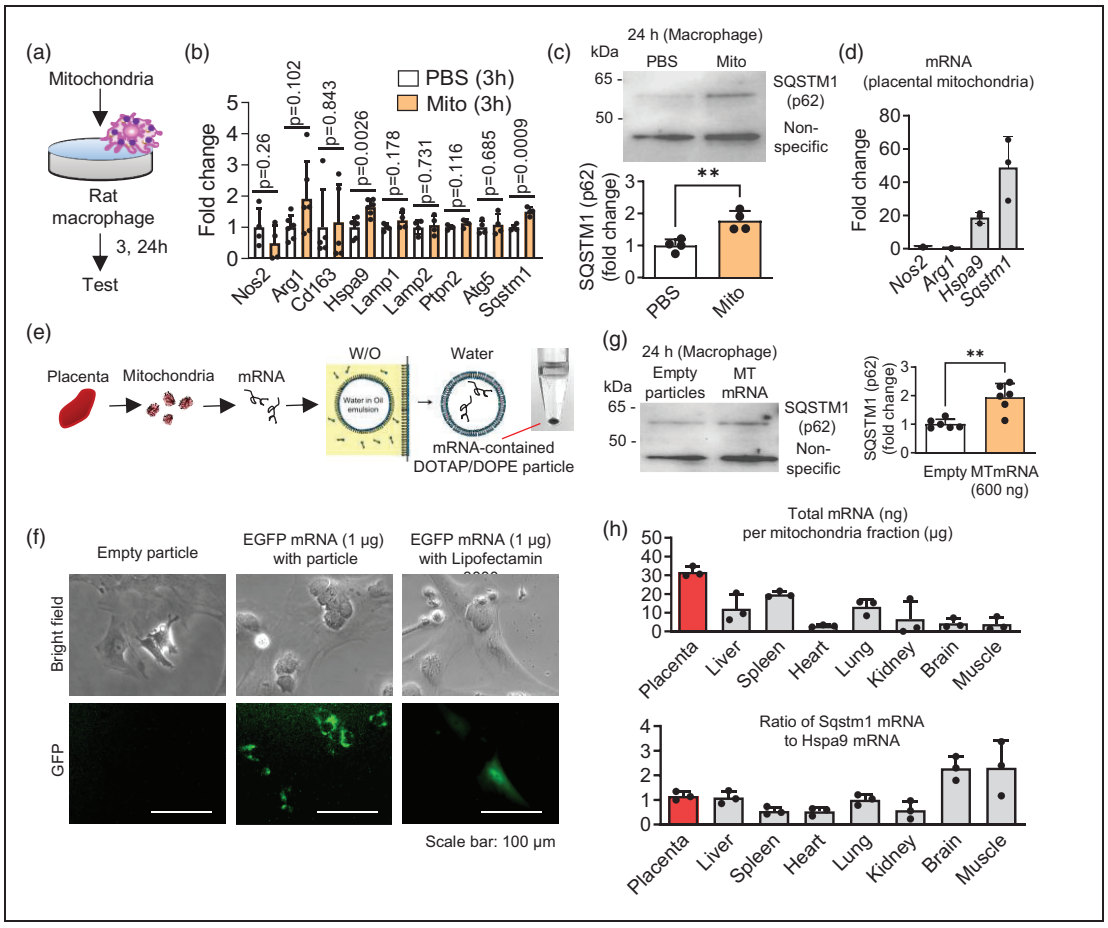

Figure 2. Mitochondria-driven SQSTM1 upregulation in macrophages. (a) Mitochondria were isolated from rat placenta and 20 μg of mitochondria fraction was added onto rat peritoneal macrophages. (b) Mitochondria treatment significantly increased gene expressions of *Hspa9*, and *Sqstm1* in macrophages at 3 hours post-treatment. $^{**}p < 0.01$, $^{***}p < 0.001$. *Nos2, Arg1, Cd163, Lamp1,* and *Lamp2* were unchanged by mitochondria treatment. (c) Western blot analysis confirmed that SQSTM1/p62 protein expression was significantly increased in macrophages at 24 h after mitochondria treatment. $^{*}p < 0.05$. (d) Mitochondria were isolated from rat placenta followed by mRNA isolation. qPCR analysis demonstrated that *Hspa9* and *Sqstm1* were detected (n = 3). (e) Mitochondria-carrying mRNA transfection strategy by using DOTAP/DOPE-encapsulation method. (f) CleanCap EGFP mRNA was first tested to evaluate transfection efficacy via DOTAP/DOPE encapsulation or lipofectamin. Twenty four hours after transfection, EGFP signal was induced by both methods. (g) Mitochondrial mRNA transfection significantly increased SQSTM1 protein in macrophages (n = 6). $^{**}p < 0.01$ and (h) mRNAs per protein and Sqstm1 ratio to Hspa9 were evaluated in various sources of mitochondria (n = 3). All data are shown as mean±SD.

was analyzed (Figure 4(c)). There were no significant differences in the number of extracellular particles with or without treatments (Figure 4(e)). But when placental mitochondria were added to macrophages, approximately 50% of extracellular mitochondria were engulfed mitochondria, whereas Rab27a inhibition clearly reduced the recycling rate by a half (Figure 4 (f) and (g)). Concomitantly, recycled mitochondria showed the highest respiratory activity in oxygen consumption analysis, whereas the inhibition of recycling exocytosis in macrophages dampened respiratory activity of extracellular mitochondria (Figure 4(h) and (i)).

Recycling exocytosis of mitochondria promotes neurite extension

Our data shows that once incorporated mitochondria are recycled and released from macrophages. But do these released mitochondria have functional relevance? To address the question, we evaluated neurite outgrowth in *in vitro* models of direct co-culture between macrophages and damaged neurons following mechanical scratch injury. Before starting the co-culture, macrophages were treated with pre-labeled placental mitochondria for 3 h and washed once to exclude free-floating mitochondria and neurons were scratched

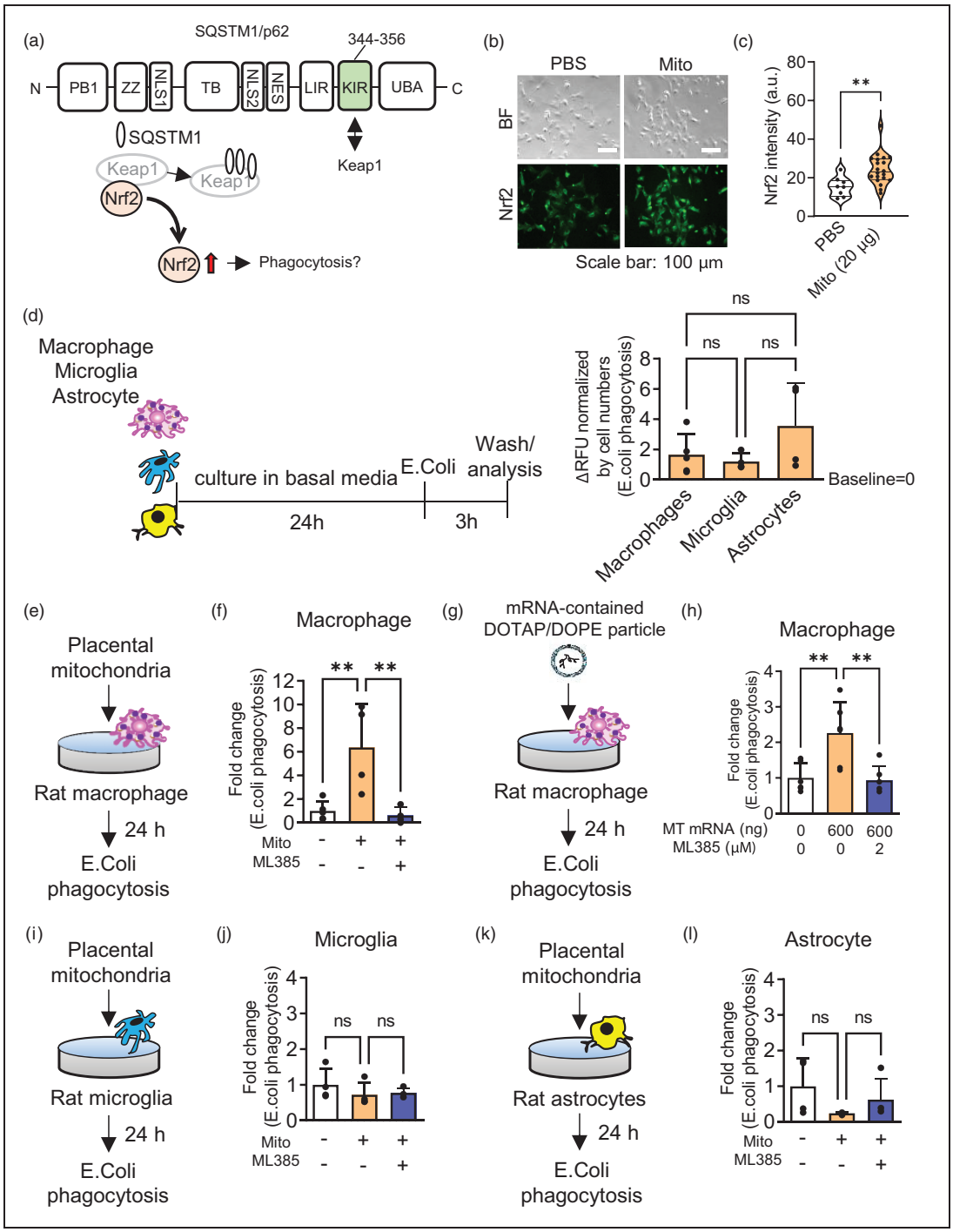

Figure 3. Mitochondria treatment increases Nrf2-mediated phagocytosis in macrophages. (a) SQSTM1 or p62 domain contains a KIR, one of the best-characterized Keap1-interacting proteins. (b) Representative images of Nrf2 expression in macrophages at 24 h post-mitochondria treatment. (c) Nrf2 intensity was significantly increased in mitochondria-treated macrophages (PBS: $n = 8$, Mito: $n = 20$). $^{**}p < 0.01$. (d) Baseline of phagocytosis activity in E.Coli particles in rat peritoneal macrophages ($n = 5$), rat primary microglia ($n = 4$), and rat primary astrocytes ($n = 4$). There was no statistically difference in the ability to incorporate E.Coli particles among cells. (e–f) Placental mitochondria (20 μg) were added onto rat peritoneal macrophages for 24 hours. Mitochondria-treated macrophages significantly increased uptake of E.Coli particles, whereas blocking Nrf2 by treatment with ML385 (2 μM) completely canceled the effect (control: $n = 5$, Mito: $n = 4$, Mito+ML385: $n = 4$). $^{**}p < 0.01$. (g–h) mRNA (600 ng), equivalent to 20 μg of whole mitochondria was encapsulated within DOTAP/DOPE-particles. Consistently, mRNA transfection increased phagocytosis but ML385 inhibited the uptake of E.Coli in macrophages ($n = 6$). $^{**}p < 0.01$. (i–j) Rat cultured microglia did not show an increase of phagocytosis after mitochondria treatment ($n = 4$) and (k–l) Rat cultured astrocytes did not increase phagocytosis after mitochondria treatment ($n = 4$). All data are shown as mean ± SD.

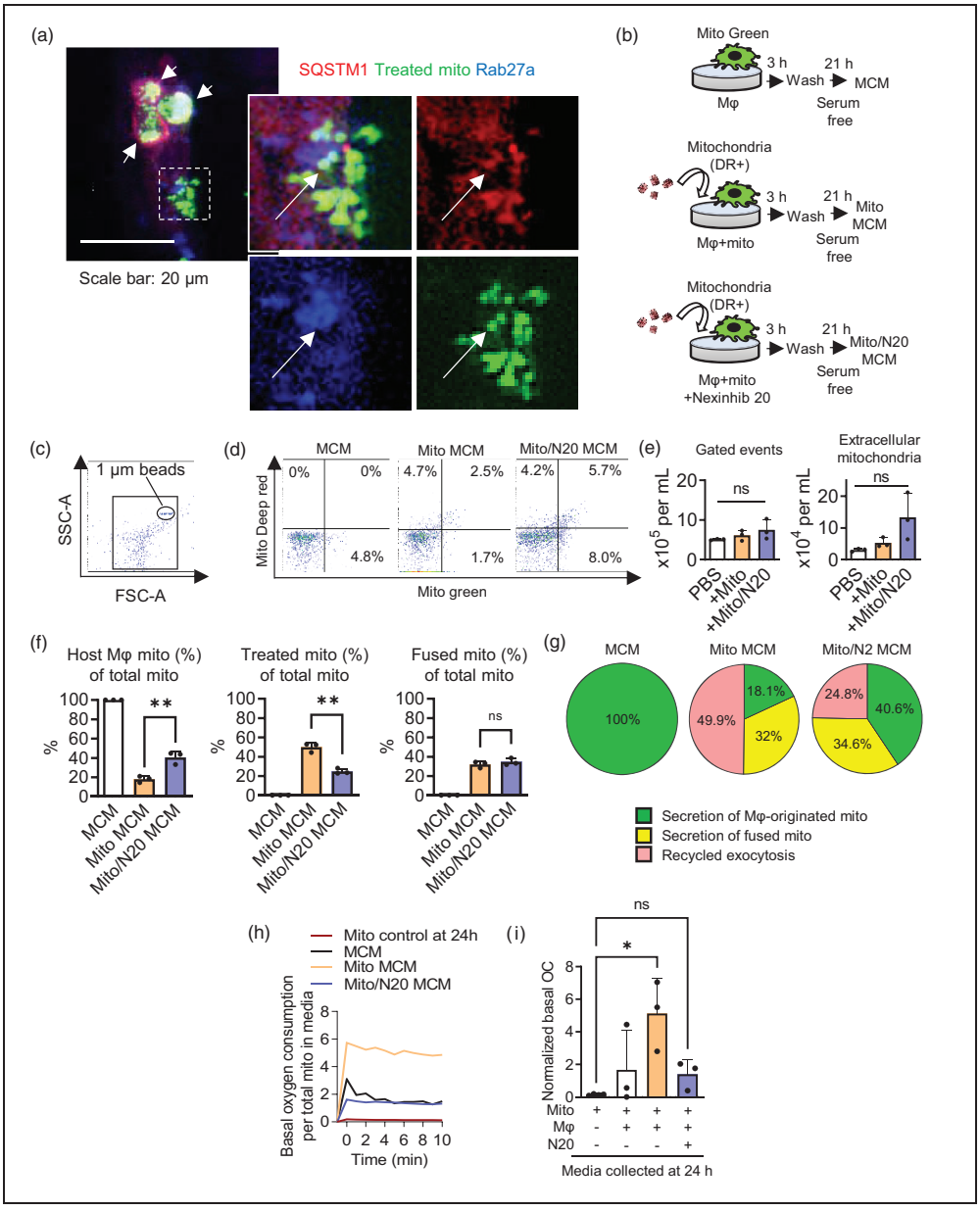

Figure 4. Engulfed mitochondrial recycling in macrophages in vitro. (a) Immunocytochemistry demonstrated that engulfed mitochondria were packed in vacuole-like vesicles expressing SQSTM1 and Rab27a in macrophages (white arrow). (b) FC analysis to calculate the percent of recycled mitochondria in macrophage-derived conditioned media. Macrophage-originated mitochondria were labeled by MitoTracker Green (100 nM) and placental mitochondria were labeled by MitoTracker Deep Red (100 nM), separately. Labeled mitochondria were added to control macrophages or Rab27a-inhibited macrophages for 3 hours followed by washing free floating mitochondria out and incubating cells with serum free media for 21 hrs. Then, macrophage-conditioned media (MCM), mitochondria-treated macrophage CM (Mito MCM), or Rab27a-inhibited macrophage with nexinhib 20 (1 μM) CM (Mito/N20 MCM) were analyzed. (c) Gating strategy using 1 μm control beads. Events less than 1 μm were analyzed. (d) Representative plots of each group. (e) Flow cytometry analysis showed that there was no difference in the number of secreted total mitochondria into culture media ($n = 3$). (f) Data analysis revealed that extracellularly released mitochondria consist of three distinct population; macrophage-originated mitochondria (only FITC+), fused mitochondria (DR+, FITC+), or treated mitochondria (only DR+). Interestingly, Rab27a inhibition promoted macrophage-originated mitochondria secretion while decreased recycling secretion of the treated mitochondria ($n = 3$). There was no difference in fused mitochondria secretion between Mito MCM and Mito/N20 MCM ($n = 3$). $^{**}p < 0.01$. (g) Under normal condition in the cultured macrophages treated with labeled mitochondria, the recycled mitochondrial secretion was approximately 50%, excluding endogenously fused mitochondria, whereas Rab27a inhibition significantly decreased the recycling secretion by a half compared to normal condition. (h) Basal oxygen consumption levels were analyzed in placental mitochondria at 24 hours post-isolation ($n = 4$), MCM ($n = 3$), Mito MCM ($n = 3$), and Mito/N20 MCM ($n = 3$). Mito MCM showed highest activity of oxygen consumption compared to other groups and (i) Recycled mitochondria in Mito MCM had the highest basal oxygen consumption [mitochondria after 24 h ($n = 4$), MCM ($n = 3$), Mito MCM ($n = 3$), and Mito/N20 MCM ($n = 3$)]. $^{*}p < 0.05$. All data are shown as mean ± SD.

to evaluate neurite extension, then partition attached on the culture dish was removed to start co-culture (Figure 5(a)). Notably, Macrophage-derived recycled mitochondria were favorably incorporated in damaged neurons compared with healthy neurons at 3 hours post-co-culture (Figure 5(b) and (c)). Interestingly, recycled mitochondria-incorporated neurons improved neurite outgrowth (Figure 5(d)–(f)), whereas neurons co-cultured with Rab27a-inhibited macrophages decreased the ability to extend neurites from the scratched injury (Figure 5(g) and (h)). Ultimately, mitochondria-treated macrophages may promote phagocytosis accompanied by recycling exocytosis of mitochondria (Figure 5(i)).

Discussion

Taken together, our proof-of-concept in vitro data suggest that (i) extracellularly added mitochondria or mRNAs extracted from mitochondrial fraction upregulates SQSTM1 in macrophages, (ii) mitochondria or mRNA treatment amplifies Nrf2-mediated phagocytosis. Finally, (iii) engulfed mitochondria are processed in Rab27a-mediated exocytosis pathway and the released mitochondria can accelerate neurite outgrowth in damaged neurons. Therefore, supplementing healthy mitochondria or mitochondria-carrying mRNAs can be engineered to target macrophage-mediated neurorecovery in CNS disorders.

Mitochondria transfer has been proposed as a new paradigm for interdependent cell-cell signaling.[16,17] As a new mitochondria-targeted therapy, therapeutic administration of mitochondria has been emerged and tested in models of various injuries or diseases.[18] What remains missing from the collective literature to date is how administered mitochondria impact immune response. Our present study provides proof-of-principle that extracellularly added mitochondria does not directly induce phenotype markers in peritoneal macrophages but increases SQSTM1 and the downstream Nrf2-mediated phagocytosis along with recycling exocytosis of engulfed mitochondria. SQSTM1 is involved in PINK1-dependent mitophagy processes including PINK1 recruitment and ubiquitin phosphorylation in depolarized mitochondria while it is not required for mitochondrial clearance.[19] Intriguingly, our study demonstrates unappreciated mechanisms driven by SQSTM1 along with Rab27a in the regulation of recycling exocytosis of incorporated mitochondria instead of mitophagy in macrophages.

Mitochondria administration has been increasingly tested. But it is important to note that there are profound limitations such as mitochondrial delivery to target cells or tissues, thus modifying mitochondria may be essential to take into account for clinical translation. It has been reported the feasibility of mitochondrial modification. For instance, Pep-1 conjugation to mitochondria improved mitochondrial delivery into dopaminergic neurons in a mouse model of Parkinson's disease.[20] Moreover, administration of polymer-functionalized mitochondria improved cellular internalization in cardiac cells.[21] Our group also attempted to encapsulate mitochondria within cationic DOTAP/DOPE-engineered liposomes and the encapsulated mitochondria improved neuroprotective efficacy in a mouse model of focal cerebral ischemia.[11] It is known that cationic liposomes promote cellular uptake in human monocytic cell line.[22] In this study, mRNAs extracted from whole placental mitochondria were successfully delivered into macrophages via DOTAP/DOPE lipid nanoparticles and enhanced phagocytic activity. Therefore, engineered encapsulation of whole mitochondria or their components such as mRNAs may be a therapeutic strategy to improve mitochondria delivery to macrophages via the peripheral administration and amplify their functions.

Nevertheless, there are a few caveats that warrant further investigation. First, our data demonstrated that isolated mitochondria from various rat organs and tissues consistently showed that extracellularly added mitochondria or their mRNAs increased SQSTM1 protein. Mitochondria have specialized mitoribosomes where translation of mitochondrial mRNAs encoded in mtDNA is carried out and SQSTM1 is, however, encoded by nuclear DNA. It has been reported that mRNA of nuclear *SOD2* gene exclusively localized to the mitochondrial surface in HeLa cells.[23] Moreover, mitochondrial complex II subunits are encoded by nuclear DNA while translated through the mitochondrial membrane,[24] implicating that some mRNAs may be present on mitochondrial surface. Further studies to dissect the mechanisms of how donor mitochondrial mRNAs are translated in recipient cells after the incorporation should be required. Second, we found *Sqstm1* mRNA in mitochondrial fractions. While our stepwise differential centrifugation method is utilized for isolating mitochondria, we acknowledge that some membrane complexes such as cytosolic ribosomes bound to mitochondria[25] and mitochondria-Endoplasmic Reticulum (ER) associated membranes along with ER-bound ribosomes[26] besides mitoribosomes may be co-isolated and the ribosome fractionation to identify the source of *Sqstm1* remains to be elucidated. Third, our hypothesis is that mitochondria treatment upregulates SQSTM1-driven Nrf2 activity, thus amplifying phagocytosis. However, mitochondria treatment amplified phagocytosis activity in macrophages but not microglia in our cell cultures and experimental conditions. It is highly possible that cellular response to mitochondria transfer can be varied, depending on

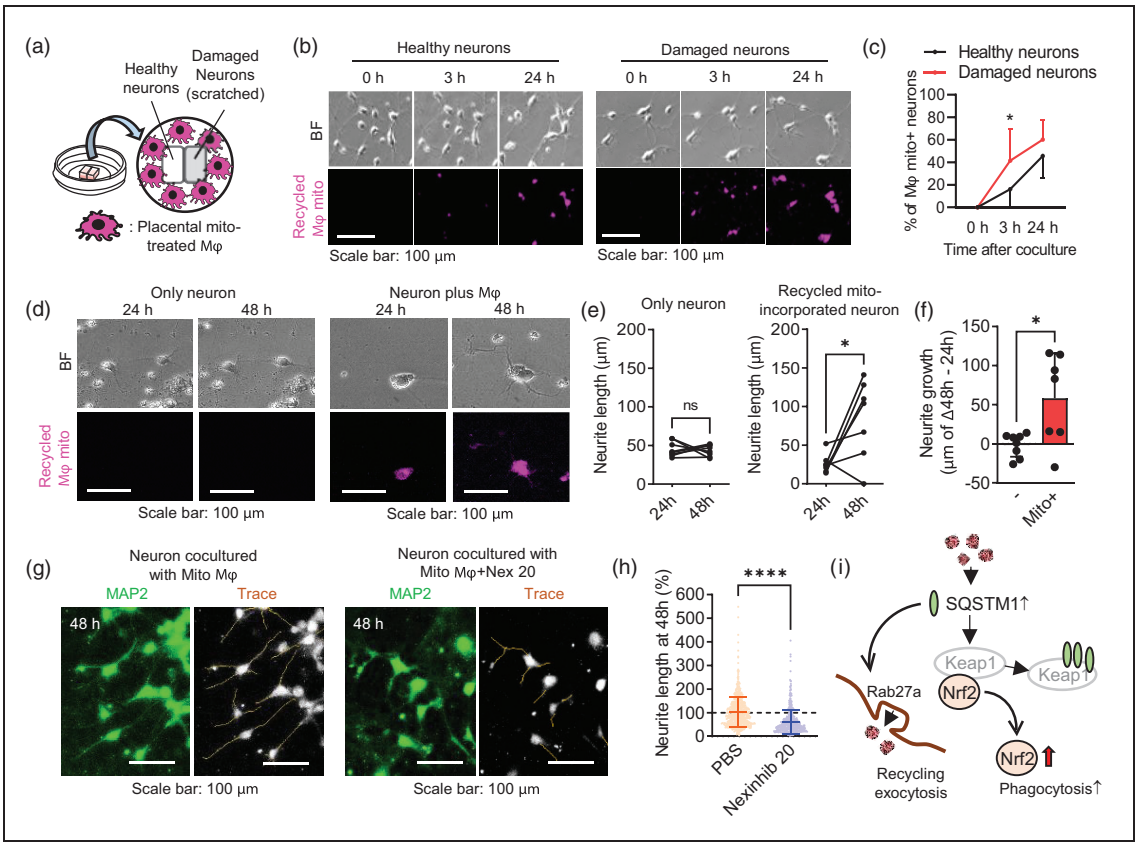

Figure 5. Mitochondria recycling for neurite extension. (a) Labeled mitochondria-treated macrophages were directly cocultured with neurons with or without scratching. (b) Fluorescence images recaptured in the same field revealed that macrophage-derived recycled mitochondria were incorporated into both healthy and scratched neurons at 3 hrs post-coculture. (c) Quantification of recycled mitochondria transfer demonstrated that injured neurons showed faster mitochondrial uptake than healthy neurons ($n = 6$). *$p < 0.05$ vs healthy neurons. (d) Fluorescence images recaptured in the same neurons revealed that recycled mitochondria-incorporated neurons appeared to extend their neurite over time. (e) Quantification of neurite length in neurons with or without recycled mitochondria incorporation (no mitochondria incorporation: $n = 8$, recycled mitochondria incorporation: $n = 7$). *$p < 0.05$. (f) Quantification of neurite growth post-mitochondria incorporation. Neurite growth was calculated in the same neurons from 24 hrs to 48 hrs co-culture. *$p < 0.05$. (g) MAP2 staining demonstrated that neurite growth was weakened, when Rab27a was inhibited by nexinhib 20 (1 μM) in macrophages. (h) Quantification of neurite length in MAP2-stained neurons. Rab27a inhibition significantly attenuated macrophage ability to extend neurites (PBS: $n = 705$ neurites, nexinhib 20: $n = 544$ neurites from 3 independent experiments and (i) Mitochondria treatment may increase SQSTM1 in macrophages followed by activating Nrf2-mediated phagocytosis accompanied by recycling exocytosis of engulfed mitochondria.

cell types. For example, macrophages uptake 20 μg of mitochondria without affecting cell viability, whereas such high amount of mitochondria induced toxicity in rat primary neurons.[11] The amount of mitochondria should be rigorously titrated to maximize microglial phagocytotic activity. Moreover, Nrf2-mediated phagocytosis is regulated by scavenger receptor, CD36 in macrophages and microglia[27] which can functionally cooperate with TLRs to enhance ligand recognition.[28] Our previous study showed macrophages but not microglia aggressively phagocytosed oligodendrocyte precursor cells via TLR4-mediated mechanisms,[29] implicating that Nrf2-mediated CD36-TLR4 in macrophages may be functionally cooperated compared with microglia. Nevertheless, the dose response to mitochondria transfer and the intracellular signaling pathways in the two phagocytes should be evaluated in future studies. Fourth, underlying molecular mechanisms of recycling exocytosis of mitochondria remain to be fully investigated. SQSTM1 is an autophagic cargo receptor and has LC3 binding domain.[30] LC3 is a well-known regulator for autophagy while the alternative function regulates an autophagy-related secretory pathway called LC3-dependent extracellular vesicle loading and secretion (LDELS), which incorporates cellular components into late endosomes and accelerates their secretion.[31] How these secretory pathways connect with Rab27a-mediated recycling pathway should be investigated. Fifth, it is intriguing that recycled mitochondria were preferentially incorporated

into mechanically damaged neurons compared with healthy neurons. It might be possible that damaged neurons send signals to adjacent macrophages so called "help-me" signals and stimulate phagocytic clearance of dead/dying cells along with recycling exocytosis in macrophages.[32,33] Additionally, damaged neurons might accelerate the incorporation of extracellular mitochondria by integrins.[7,34] Ultimately, future studies are warranted to dissect the mechanisms of cell-to-cell interaction required for phagocytosis and recycling exocytosis of mitochondria in macrophages in the context of CNS injury. Finally, our data showed that recycled mitochondria in macrophages were transferred to other cell type such as neurons. However, the beneficiality of mitochondria transfer depends on the context. For example, neuroglial interaction via fragmented dysfunctional mitochondria transfer may cause neurodegeneration.[35] Therefore, it should be useful to ask whether therapeutic administration of mitochondria can improve mitochondrial functional status in macrophages to prevent deleterious mitochondria recycling under pathophysiological conditions in the CNS.

Crosstalk between brain and systemic responses may be important. For example, blood monocytes/macrophages are a source of brain perivascular macrophages[36] and regulate functional recovery in the CNS.[37] Within the emerging paradigm of extracellular mitochondria transfer, our study suggests that mitochondria treatment upregulates macrophage-mediated phagocytosis and recycling exocytosis of mitochondria that may promote neuroplasticity in injured neurons. Further studies are warranted to investigate whether these mechanisms can be manipulated for therapeutic gain in CNS disorders.

Funding

The author(s) disclosed receipt of the following financial support for the research, authorship, and/or publication of this article: This work was supported by NIH and MGH ECOR Interim Support Fund.

Acknowledgements

We thank NIH and MGH ECOR Interim Support Fund for funding support. Cytometric findings reported here were performed in the MGH Department of Pathology Flow and Image Cytometry Research Core. The authors thank Eng H. Lo for many helpful discussions.

Declaration of conflicting interests

The author(s) declared no potential conflicts of interest with respect to the research, authorship, and/or publication of this article.

Authors' contributions

M.T., S.I., D.B.B., E.L., F.Z., J.H.P., E.E., G.P., T.N., Y.N. contributed to conducted experiments and data analysis. K.H. contributed to experimental design and manuscript preparation.

ORCID iDs

Masayoshi Tanaka https://orcid.org/0009-0000-1222-7390
Ester Licastro https://orcid.org/0000-0001-6917-4605
Takafumi Nakano https://orcid.org/0000-0001-5667-1979
Kazuhide Hayakawa https://orcid.org/0000-0002-1229-2413

References

1. Tait SW and Green DR. Mitochondria and cell signalling. *J Cell Sci* 2012; 125: 807–815.
2. Devine MJ and Kittler JT. Mitochondria at the neuronal presynapse in health and disease. *Nat Rev Neurosci* 2018; 19: 63–80.
3. Lesnik C, Golani-Armon A and Arava Y. Localized translation near the mitochondrial outer membrane: an update. *RNA Biol* 2015; 12: 801–809.
4. Spees JL, Olson SD, Whitney MJ, et al. Mitochondrial transfer between cells can rescue aerobic respiration. *Proc Natl Acad Sci U S A* 2006; 103: 1283–1288.
5. Dong LF, et al. Mitochondria on the move: horizontal mitochondrial transfer in disease and health. *J Cell Biol* 2023; 222
6. Brestoff JR, Wilen CB, Moley JR, et al. Intercellular mitochondria transfer to macrophages regulates white adipose tissue homeostasis and is impaired in obesity. *Cell Metab* 2021; 33: 270–282 e278.
7. Hayakawa K, Esposito E, Wang X, et al. Transfer of mitochondria from astrocytes to neurons after stroke. *Nature* 2016; 535: 551–555.
8. Stephens OR, Grant D, Frimel M, et al. Characterization and origins of cell-free mitochondria in healthy murine and human blood. *Mitochondrion* 2020; 54: 102–112.
9. Al Amir Dache Z, Otandault A, Tanos R, et al. Blood contains circulating cell-free respiratory competent mitochondria. *FASEB J* 2020; 34: 3616–3630.
10. Nakamura Y, Lo EH and Hayakawa K. Placental mitochondria therapy for cerebral ischemia-reperfusion injury in mice. *Stroke* 2020; 51: 3142–3146.
11. Nakano T, Nakamura Y, Park JH, et al. Mitochondrial surface coating with artificial lipid membrane improves the transfer efficacy. *Commun Biol* 2022; 5: 745.
12. Kumar AV, Mills J and Lapierre LR. Selective autophagy receptor p62/SQSTM1, a pivotal player in stress and aging. *Front Cell Dev Biol* 2022; 10: 793328.
13. Harvey CJ, Thimmulappa RK, Sethi S, et al. Targeting Nrf2 signaling improves bacterial clearance by alveolar macrophages in patients with COPD and in a mouse model. *Sci Transl Med* 2011; 3: 78ra32.
14. Braun V and Niedergang F. Linking exocytosis and endocytosis during phagocytosis. *Biol Cell* 2006; 98: 195–201.

15. Solvik TA, Nguyen TA, Tony Lin Y-H, et al. Secretory autophagy maintains proteostasis upon lysosome inhibition. *J Cell Biol* 2022; 221
16. Gollihue JL and Rabchevsky AG. Prospects for therapeutic mitochondrial transplantation. *Mitochondrion* 2017; 35: 70–79.
17. Hayakawa K, Bruzzese M, Chou SH-Y, et al. Extracellular mitochondria for therapy and diagnosis in acute central nervous system injury. *JAMA Neurol* 2018; 75: 119–122.
18. Nakamura Y, Park JH and Hayakawa K. Therapeutic use of extracellular mitochondria in CNS injury and disease. *Exp Neurol* 2020; 324: 113114.
19. Poon A, Saini H, Sethi S, et al. The role of SQSTM1 (p62) in mitochondrial function and clearance in human cortical neurons. *Stem Cell Reports* 2021; 16: 1276–1289.
20. Chang J-C, Wu S-L, Liu K-H, et al. Allogeneic/xenogeneic transplantation of peptide-labeled mitochondria in Parkinson's disease: restoration of mitochondria functions and attenuation of 6-hydroxydopamine-induced neurotoxicity. *Transl Res* 2016; 170: 40–56.e43.
21. Wu S, Zhang A, Li S, et al. Polymer functionalization of isolated mitochondria for cellular transplantation and metabolic phenotype alteration. *Adv Sci (Weinh)* 2018; 5: 1700530.
22. Giulimondi F, Digiacomo L, Pozzi D, et al. Interplay of protein corona and immune cells controls blood residency of liposomes. *Nat Commun* 2019; 10: 3686.
23. Kaltimbacher V, Bonnet C, Lecoeuvre G, et al. mRNA localization to the mitochondrial surface allows the efficient translocation inside the organelle of a nuclear recoded ATP6 protein. *RNA* 2006; 12: 1408–1417.
24. Schulz C, Schendzielorz A and Rehling P. Unlocking the presequence import pathway. *Trends Cell Biol* 2015; 25: 265–275.
25. Gold VA, Chroscicki P, Bragoszewski P, et al. Visualization of cytosolic ribosomes on the surface of mitochondria by electron cryo-tomography. *EMBO Rep* 2017; 18: 1786–1800.
26. Gemmer M, Chaillet ML, van Loenhout J, et al. Visualization of translation and protein biogenesis at the ER membrane. *Nature* 2023; 614: 160–167.
27. Grajchen E, Wouters E, van de Haterd B, et al. CD36-mediated uptake of myelin debris by macrophages and microglia reduces neuroinflammation. *J Neuroinflammation* 2020; 17: 224.
28. Lee CC, Avalos AM and Ploegh HL. Accessory molecules for toll-like receptors and their function. *Nat Rev Immunol* 2012; 12: 168–179.
29. Hayakawa K, Pham L-DD, Seo JH, et al. CD200 restrains macrophage attack on oligodendrocyte precursors via toll-like receptor 4 downregulation. *J Cereb Blood Flow Metab* 2016; 36: 781–793.
30. Pankiv S, Clausen TH, Lamark T, et al. p62/SQSTM1 binds directly to Atg8/LC3 to facilitate degradation of ubiquitinated protein aggregates by autophagy. *J Biol Chem* 2007; 282: 24131–24145.
31. Leidal AM, Huang HH, Marsh T, et al. The LC3-conjugation machinery specifies the loading of RNA-binding proteins into extracellular vesicles. *Nat Cell Biol* 2020; 22: 187–199.
32. Zhang W, Zhao J, Wang R, et al. Macrophages reprogram after ischemic stroke and promote efferocytosis and inflammation resolution in the mouse brain. *CNS Neurosci Ther* 2019; 25: 1329–1342.
33. Xing C and Lo EH. Help-me signaling: non-cell autonomous mechanisms of neuroprotection and neurorecovery. *Prog Neurobiol* 2017; 152: 181–199.
34. Wu X and Reddy DS. Integrins as receptor targets for neurological disorders. *Pharmacol Ther* 2012; 134: 68–81.
35. Joshi AU, Minhas PS, Liddelow SA, et al. Fragmented mitochondria released from microglia trigger A1 astrocytic response and propagate inflammatory neurodegeneration. *Nat Neurosci* 2019; 22: 1635–1648.
36. Kim W-K, Alvarez X, Fisher J, et al. CD163 identifies perivascular macrophages in normal and viral encephalitic brains and potential precursors to perivascular macrophages in blood. *Am J Pathol* 2006; 168: 822–834.
37. Wattananit S, Tornero D, Graubardt N, et al. Monocyte-derived macrophages contribute to spontaneous long-term functional recovery after stroke in mice. *J Neurosci* 2016; 36: 4182–4195.